J. Fluid Mech. (1983), *vol.* 127, *pp.* 283–297
Printed in Great Britain

Free-surface flow over a semicircular obstruction, including the influence of gravity and surface tension

By LAWRENCE K. FORBES†
Applied Mathematics Department, University of Adelaide, South Australia 5000

(Received 8 October 1981 and in revised form 24 August 1982)

A previous study by Forbes & Schwartz (1982) on flow under gravity of a fluid over a submerged semicircular disturbance is generalized to include the effects of surface tension. A linearized theory is presented, in which the existence of three different branches of solution is predicted. The solution of the fully nonlinear problem by a boundary-integral technique supports this prediction. The wave resistance experienced by the obstacle is computed for the linearized and nonlinear theories.

1. Introduction

The flow of an ideal fluid with a free surface over a submerged semicircular cylinder affixed to the bed of a running stream was recently considered by Forbes & Schwartz (1982). A linearized theory was developed for the case in which the radius of the disturbing semicircular cylinder is small, whilst for cylinders of arbitrary radius, the solution of the fully nonlinear problem was effected utilizing an efficient boundary-integral technique. Both the linearized and nonlinear results indicated the existence of two different branches of solution to this problem, although in the nonlinear case these two branches may possibly overlap, so that for certain values of the upstream Froude number either type of solution is a likely outcome.

Fluid flow over various bottom topographies has attracted considerable attention throughout the history of fluid mechanics, and the literature on the topic is extensive. Lamb (1932, p. 409) presents a general linearized theory for flow over stream beds of 'arbitrary' shape; however, it was pointed out by Forbes & Schwartz (1982) that Lamb's theory ceases to be valid when stagnation points are present on the bottom, since the assumptions of the theory are violated at these points. This theory is reviewed by Wehausen & Laitone (1960, p. 569), who also discuss free-surface flow over a step discontinuity in the stream bed. More recently, a linearized theory for flow over certain bottom profiles was developed by Gazdar (1973).

Nonlinear potential flows over bottom-mounted obstacles, in the absence of surface tension, have also been considered recently. Forbes (1981*a*, *b*) investigated the flow over a submerged semi-elliptical body, and demonstrated that the nonlinear drag force on the obstacle could be made to vanish for special body shapes in subcritical flow. Aitchison (1979) employed a variable finite-element technique to solve for flow over a triangular weir. In addition to the two nonlinear branches of solution obtained by Forbes & Schwartz (1982), she obtained a third nonlinear family of solutions, in which the flow upstream of the obstacle is subcritical, but becomes supercritical downstream. The finite-difference scheme employed by von Kerczek & Salvesen (1977) and the boundary-fitting finite-difference schemes of Haussling &

† Present address: Institute of Hydraulic Research, The University of Iowa, Iowa City, Iowa 52242, U.S.A.

Coleman (1977) and Shanks & Thompson (1977) may presumably also be applied to the solution of flow problems involving irregular bottom topographies, although this does not yet appear to have been attempted.

In addition to work on nonlinear wave motion under the influence of gravity, such as the investigations of Schwartz (1974) and Cokelet (1977), there is currently considerable interest in nonlinear wave motion under the combined effects of gravity and surface tension. Schwartz & Vanden Broeck (1979) solved this problem using a boundary-integral technique, and investigated the role of 'Wilton's ripples' in the mathematical structure of the solution. Their results indicate the existence of apparently infinitely many families of solutions to this problem, where the free surface for solutions of a particular family type possesses a characteristic number of surface-tension ripples 'riding' on the overall wave profile. Alternative analyses of this problem have been undertaken by Hogan (1979, 1980) and Chen & Saffman (1979, 1980).

In the present paper we consider the nonlinear problem of fluid flow over a semicircular cylinder attached to the bed of a running stream, when both gravity and surface tension are present. The problem is formulated and solved, as in Forbes & Schwartz (1982), utilizing a boundary-integral technique in an inverse plane in which the velocity potential and stream function are the independent variables. A preliminary conformal mapping is performed, which both ensures that the fluid behaviour at the two stagnation points on the semicircular cylinder is correctly represented, and eliminates the necessity to place numerical grid points along the bottom. The nonlinear results discussed in this paper summarize the outcomes of approximately 200 numerically computed free-surface profiles; this is by no means sufficient to completely describe the properties of the solutions to this problem, although some general trends may be observed.

2. Formulation

Consider steady, two-dimensional flow of an ideal fluid in a stream in which has been placed a semicircular cylinder of radius R_c, with its centre at the origin of a coordinate system in which the y-axis points vertically. In the absence of surface tension, the flow far upstream is uniform with velocity c in the positive x-direction, and depth H. The surface tension of the fluid is τ, and g is the downward acceleration due to gravity.†

Dimensionless variables are defined by referring all lengths to the quantity H, and all velocities to c. The velocity potential ϕ and stream function ψ are normalized with respect to the product cH, so that the bottom is the streamline $\psi = 0$ and the surface is $\psi = 1$, in dimensionless variables. The non-dimensional flow is depicted in figure 1.

The three dimensionless parameters of the problem are the depth-based Froude number

$$F = c/(gH)^{\frac{1}{2}},$$

the dimensionless circle radius

$$\alpha = R_c/H,$$

and the surface-tension number

$$T = \tau/\rho g H^2,$$

where ρ is the density of the fluid.

† When surface tension is present, a wavetrain may appear upstream of the semicircle. In this case the reference speed c and depth H are defined at points of zero curvature of the free surface far upstream, by (2.2).

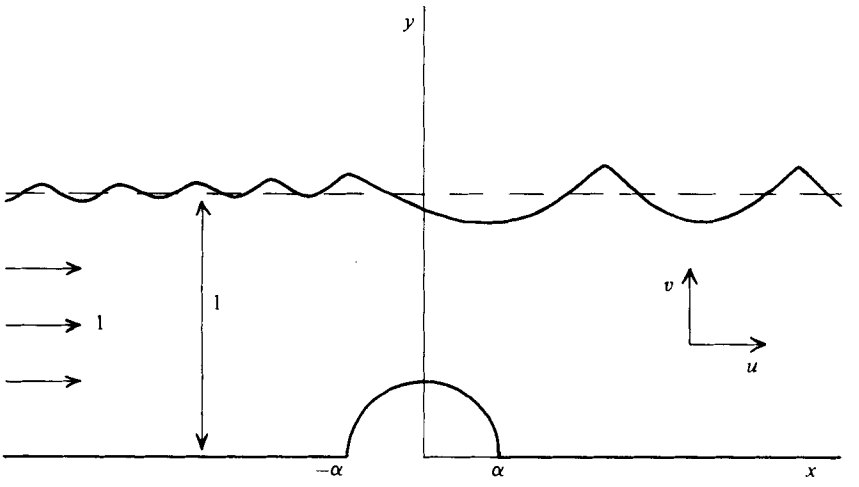

FIGURE 1. The non-dimensional flow situation and coordinates in the z-plane.

Since the fluid is incompressible and flows irrotationally, it follows that the quantities ϕ and ψ obey the Cauchy–Riemann equations in the fluid interior. The complex variable $f = \phi + i\psi$ may therefore be expressed as an analytic function of the variable $z = x + iy$. The conjugate complex velocity w is defined by the expression

$$w = u - iv = \frac{df}{dz},$$

where u and v are respectively the horizontal and vertical components of the velocity vector.

The requirement that there be no flow normal to the bottom streamline $y = h(x)$ results in the equation

$$u\frac{dh}{dx} = v \quad \text{on} \quad y = h(x), \tag{2.1}$$

where

$$h(x) = \begin{cases} (\alpha^2 - x^2)^{\frac{1}{2}} & (|x| \leqslant \alpha) | \leqslant \alpha), \\ 0 & (|x| \geqslant \alpha). \end{cases}$$

At the free surface of the fluid the Bernoulli equation may be written

$$\tfrac{1}{2}F^2(u^2 + v^2) + y - \frac{T}{R} = \tfrac{1}{2}F^2 + 1, \tag{2.2}$$

where R is the local radius of curvature of the surface and is defined as

$$\frac{1}{R} = \left[\left(\frac{d^2x}{ds^2}\right)^2 + \left(\frac{d^2y}{ds^2}\right)^2\right]^{\frac{1}{2}}.$$

Here s is the arclength along the surface, so that $ds^2 = dx^2 + dy^2$.

Following Forbes & Schwartz (1982), the problem is reformulated in a ζ-plane, in which the bottom is simply a straight line, free of stagnation points. The new variable $\zeta = \xi + i\eta$ is related to $z = x + iy$ by the Joukowski transformation

$$z = \zeta + (\zeta^2 - \alpha^2)^{\frac{1}{2}}. \tag{2.3}$$

In the ζ-plane the bottom condition (2.1) takes the simple form

$$\phi_\eta = 0 \quad \text{on} \quad \eta = 0, \tag{2.4}$$

where the subscript denotes partial differentiation. The Bernoulli equation (2.2) at the free surface may be written

$$\tfrac{1}{8}F^2\frac{(z^2-\alpha^2)(\bar{z}^2-\alpha^2)}{(z\bar{z})^2}(\phi_\xi^2+\phi_\eta^2)+\operatorname{Im}\{z\}-\tfrac{1}{2}F^2-1$$
$$-T\frac{2(z\bar{z})}{(z^2-\alpha^2)^{\frac{1}{2}}(\bar{z}^2-\alpha^2)^{\frac{1}{2}}}\left\{\zeta_{ss}\bar{\zeta}_{ss}-\alpha^2\bar{\zeta}_s^2\zeta_{ss}\frac{4\bar{z}}{(\bar{z}^2-\alpha^2)^2}\right.$$
$$\left.-\alpha\zeta_s^2\bar{\zeta}_{ss}\frac{4z}{(z^2-\alpha^2)^2}+\alpha^4\zeta_s^2\bar{\zeta}_s^2\frac{16(z\bar{z})}{(z^2-\alpha^2)^2(\bar{z}^2-\alpha^2)^2}\right\}^{\frac{1}{2}}=0. \quad (2.5)$$

The bars denote complex conjugation.

Finally, the roles of the variables f and ζ are interchanged, so that the quantity $\zeta=\xi+i\eta$ is sought as an analytic function of the independent variable $f=\phi+i\psi$. This transformation, due to Stokes (1880), simplifies the problem to the extent that the free surface in the f-plane has the known location $\psi=1$, although its position in the ζ-plane is unknown.

In the f-plane the bottom condition (2.4) becomes

$$\eta=0 \quad \text{on} \quad \psi=0, \quad (2.6)$$

and the Bernoulli equation (2.5) takes the form

$$\tfrac{1}{8}F^2\frac{(z^2-\alpha^2)(\bar{z}^2-\alpha^2)}{(z\bar{z})^2(\zeta_\phi\bar{\zeta}_\phi)}+\operatorname{Im}\{z\}-\tfrac{1}{2}F^2-1$$
$$-\tfrac{1}{4}iT\frac{(z^2-\alpha^2)^{\frac{1}{2}}(\bar{z}^2-\alpha^2)^{\frac{1}{2}}}{(z\bar{z})(\zeta_\phi\bar{\zeta}_\phi)^{\frac{3}{2}}}\left\{(\zeta_\phi\bar{\zeta}_{\phi\phi}-\bar{\zeta}_\phi\zeta_{\phi\phi})\right.$$
$$\left.+4\alpha^2(\zeta_\phi\bar{\zeta}_\phi)\left[\frac{z\zeta_\phi}{(z^2-\alpha^2)^2}-\frac{\bar{z}\bar{\zeta}_\phi}{(\bar{z}^2-\alpha^2)^2}\right]\right\}=0 \quad \text{on} \quad \psi=1. \quad (2.7)$$

The function $z(\zeta)$ may be obtained from (2.3).

Equation (2.7) provides one relation between the real and imaginary parts of the function $\zeta(f)$ at the free surface $\psi=1$. A second relation between them has been derived by Forbes & Schwartz (1982) using the Cauchy Integral Theorem. Thus

$$[\xi_\phi(\phi,1)-\tfrac{1}{2}]-\frac{2}{\pi}\int_{-\infty}^{\infty}[\xi_\theta(\theta,1)-\tfrac{1}{2}]\frac{d\theta}{(\theta-\phi)^2+4}$$
$$=-\frac{1}{\pi}\left\{\int_{-\infty}^{\infty}\frac{\eta_\theta(\theta,1)\,d\theta}{\theta-\phi}+\int_{-\infty}^{\infty}\frac{\eta_\theta(\theta,1)(\theta-\phi)\,d\theta}{(\theta-\phi)^2+4}\right\}. \quad (2.8)$$

Equation (2.8) is a consequence of the analyticity of the function $\zeta(f)$, and includes the bottom condition (2.6) implicitly.

In order to specify the problem completely, some knowledge of the solution infinitely far upstream must be assumed. In the absence of surface tension, this reduces to the radiation condition

$$\zeta\to\tfrac{1}{2}f \quad \text{as} \quad \phi\to-\infty. \quad (2.9)$$

The more general case in which surface tension is present will be discussed in §5.

The free-surface profile is thus obtained parametrically in the form $(\xi(\phi,1),\eta(\phi,1))$ by the solution of (2.7) and (2.8), together with a condition of the type (2.9). The original variables x and y are then recovered from (2.3).

The drag force D acting per unit length of the semicircular cylinder is calculated by integrating the pressure p across its surface. Here p and D have been made dimensionless by reference to the quantities ρgH and ρgH^2 respectively. Thus

$$D = \int_{-\alpha}^{\alpha} ph'(x)\,dx = \tfrac{1}{2}F^2 \int_{-\alpha}^{\alpha} (u^2+v^2)\frac{x}{(\alpha^2-x^2)^{\frac{1}{2}}}dx.$$

In the ζ-plane this equation becomes

$$D = \frac{1}{2}\frac{F^2}{\alpha^2}\int_{-\alpha}^{\alpha} \xi(\alpha^2-\xi^2)^{\frac{1}{2}}\left(\frac{\partial\phi}{\partial\xi}\right)^2_{\eta=0} d\xi. \tag{2.10}$$

When transformed into the f-plane, (2.10) takes the form

$$D = \frac{1}{2}\frac{F^2}{\alpha^2}\int_{\phi_{-\alpha}}^{\phi_{+\alpha}} \frac{\xi(\alpha^2-\xi^2)^{\frac{1}{2}}}{\xi_\phi} d\phi, \tag{2.11}$$

where the quantities $\phi_{\pm\alpha}$ are the solutions to the equations

$$\xi(\phi_{\pm\alpha}, 0) = \pm\alpha. \tag{2.12}$$

The function $\xi(\phi, 0)$ at the bottom $\psi = 0$ is obtained from the previously computed solution $\xi(\phi, 1)$ at the free surface by means of the Cauchy Integral Theorem.

3. The linearized solution

When the square of the circle radius, α^2, is a small quantity, a linearized theory may be developed by expanding the solution $\zeta(f)$ in the regular perturbation series

$$\zeta(f) = \tfrac{1}{2}f + \alpha^2 \mathscr{F}_1(f) + O(\alpha^4). \tag{3.1}$$

Equation (3.1) is substituted into the full nonlinear equations of motion, and only terms of first order in α^2 are retained. Thus the Bernoulli equation (2.7) yields the linearized free-surface condition

$$\mathrm{Re}\left\{-iT\frac{d^2\mathscr{F}_1}{df^2} + F^2\frac{d\mathscr{F}_1}{df} + i\mathscr{F}_1\right\} = T\frac{1-3\phi^2}{(\phi^2+1)^3} + \tfrac{1}{2}F^2\frac{1-\phi^2}{(\phi^2+1)^2} + \frac{1}{2}\frac{1}{\phi^2+1} \quad \text{on} \quad \psi = 1. \tag{3.2}$$

The solution is sought as a Fourier transform, with the integrand chosen to satisfy the bottom condition $\mathrm{Im}\{\mathscr{F}_1\} = 0$ on $\psi = 0$. Thus

$$\mathscr{F}_1(f) = \int_0^\infty C(\kappa)\sin\kappa f\,d\kappa. \tag{3.3}$$

The real function $C(\kappa)$ is determined by substitution into (3.2), and may be written

$$C(\kappa) = \frac{1}{2}\frac{e^{-\kappa}(T\kappa^2 + F^2\kappa + 1)}{\kappa F^2\cosh\kappa - (1+\kappa^2 T)\sinh\kappa}.$$

It is evident that the function $C(\kappa)$ may become singular at a maximum of two positive real values of κ. Let these values be κ_0 and κ_1, and define $\kappa_0 < \kappa_1$; then κ_0 and κ_1 are the solutions to the dispersion relation

$$d(\kappa_i) = (1+\kappa_i^2 T)\tanh\kappa_i - \kappa_i F^2 = 0 \quad (i = 0, 1). \tag{3.4}$$

If either κ_0 or κ_1 exists, the function $\mathscr{F}_1(f)$ in (3.3) becomes indeterminate, since the integral on the right-hand side of this equation fails to have meaning in the usual

sense. In this case the integral is interpreted as a contour integral in the complex κ-plane, with the path of integration passing below the pole singularity at κ_0 and above the singularity at κ_1 in semicircles of vanishingly small radius. The solution (3.1) may therefore be written

$$\zeta(f) = \tfrac{1}{2}f + \tfrac{1}{2}\alpha^2\left\{\int_0^\infty \frac{e^{-\kappa}(T\kappa^2 + F^2\kappa + 1)\sin\kappa f}{\kappa F^2\cosh\kappa - (1+\kappa^2 T)\sinh\kappa}\,d\kappa \right.$$
$$+ \frac{\pi e^{-\kappa_0}(T\kappa_0^2 + F^2\kappa_0 + 1)\cos(\kappa_0 f)}{\left[F^2 - (1+\kappa_0^2 T) + \dfrac{\kappa_0^2 F^2(F^2-2T)}{1+\kappa_0^2 T}\right]\cosh\kappa_0}$$
$$\left. - \frac{\pi e^{-\kappa_1}(T\kappa_1^2 + F^2\kappa_1 + 1)\cos\kappa_1 f}{\left[F^2 - (1+\kappa_1^2 T) + \dfrac{\kappa_1^2 F^2(F^2-2T)}{1+\kappa_1^2 T}\right]\cosh\kappa_1}\right\} + O(\alpha^4). \tag{3.5}$$

When either κ_0 or κ_1 fails to exist, the term involving that quantity should be omitted from (3.5).

Three distinct, different branches of solution are predicted by the linearized theory, and for convenience will be referred to in this paper as solutions of types 1, 2 and 3. Solutions of type 1 exist only when $F < 1$, and possess a train of gravity waves downstream, and capillary waves upstream of the semicircle, since both κ_0 and κ_1 exist in this case. Solutions of type 2 occur at large values of the surface-tension parameter T, and are also confined to the subcritical regime $F < 1$. In this case, however, there are no waves either upstream or downstream of the semicircle, and the free surface is symmetric about the y-axis and possesses a local depression above the semicircle, since neither κ_0 nor κ_1 exist. Type 3 solutions occur only in the supercritical regime $F > 1$, and the transcendental equation (3.4) possesses the single real root κ_1 for these solutions. Thus, the free surface consists of a train of capillary waves upstream followed by a rise above the semicircular obstruction.

The regions in the parameter space (F, T) in which the various branches of the linearized solution exist are sketched in figure 2. The solid curves in this diagram are the boundaries between regions in which different solution types occur. There is no solution when the parameters F and T describe a point on these curves, since the two roots of the transcendental equation (3.4) coalesce, so that $\kappa_0 = \kappa_1 = \kappa^*$, and the integral in (3.5) fails to exist. The location of these curves is found by solving the system of equations

$$d(\kappa^*) = (1+\kappa^{*2}T)\tanh\kappa^* - \kappa^* F^2 = 0,$$
$$d'(\kappa^*) = 2\kappa^* T\tanh\kappa^* + (1+\kappa^{*2}T)\operatorname{sech}^2\kappa^* - F^2 = 0.$$

These equations enable the quantities κ^* and T to be obtained for a particular value of F.

The drag force D experienced by the semicircular obstruction is calculated for the linearized solution by inverting (3.5), to obtain a relation of the form $f(\zeta)$, and then substituting into (2.10). This results in the expression

$$D = \tfrac{1}{4}A_1^{(+)2}\left[1 - \kappa_0^2 T - (1+\kappa_0^2 T)\frac{2\kappa_0}{\sinh 2\kappa_0}\right]$$
$$- \tfrac{1}{4}A_1^{(-)2}\left[1 - \kappa_1^2 T - (1+\kappa_1^2 T)\frac{2\kappa_1}{\sinh 2\kappa_1}\right] + O(\alpha^5). \tag{3.6}$$

The quantities $A_1^{(+)}$ and $A_1^{(-)}$ are the linearized amplitudes of the wavetrains far

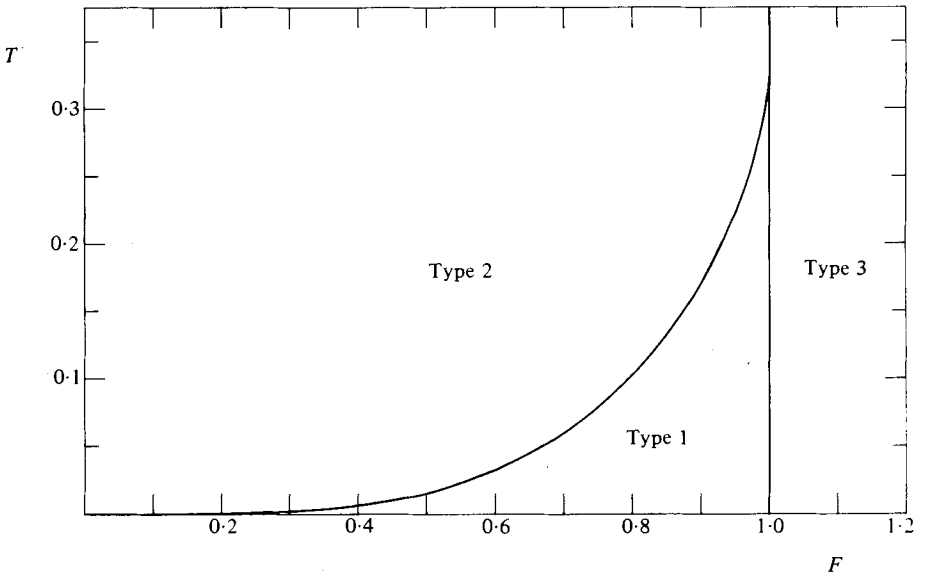

FIGURE 2. The regions in which the three branches of the linearized solution exist.

downstream and far upstream respectively, when these exist. Their values may be obtained from (3.5) by means of the usual asymptotic analysis. Thus for solutions of type 1

$$y \to 1 - A_1^{(+)} \sin \kappa_0 x + O(\alpha^4) \quad \text{as} \quad x \to +\infty,$$

$$y \to 1 + A_1^{(-)} \sin \kappa_1 x + O(\alpha^4) \quad \text{as} \quad x \to -\infty,$$

where

$$A_1^{(+)} = A_1(\kappa_0), \quad A_1^{(-)} = A_1(\kappa_1),$$

$$A_1(\kappa) = \frac{2\alpha^2 F^2 \pi \kappa}{\left[F^2 - (1+\kappa^2 T) + \dfrac{\kappa^2 F^2 (F^2 - 2T)}{1+\kappa^2 T}\right] \cosh \kappa}.$$

As the boundary between solutions of type 1 and type 2 shown in figure 2 is approached, the two wavenumbers κ_0 and κ_1 coalesce, and the wave amplitudes $A_1^{(+)}$ and $A_1^{(-)}$ both become infinite. The drag D also becomes unbounded when $\kappa_0 = \kappa_1 = \kappa^*$, but drops abruptly to zero for solutions of type 2, since in this case there are no waves formed in the far field.

4. Numerical methods

The numerical scheme for the solution of the nonlinear system of equations (2.7) and (2.8), together with a relation of the form (2.9), at the $N+1$ equally spaced free-surface points ϕ_0, $\phi_1, \ldots, \phi_N$ has been described in principle by Forbes & Schwartz (1982). Accordingly, only a brief outline of the process need be provided here.

To begin, the integrodifferential equation (2.8) is truncated upstream and downstream at the points ϕ_0 and ϕ_N. The treatment of the Cauchy principal-value integral is standard, and consists of rendering the integral non-singular by subtracting the singular part and integrating it explicitly. In order to satisfy an upstream condition of the type (2.9) it is assumed that the values of all the flow variables are given at

the first point ϕ_0; usually the quantities ξ_0, η_0, η_0', ξ_0'' and η_0'' are taken from the linearized solution, and the Bernoulli equation at the first point gives ξ_0'. The integrodifferential equation is evaluated at the midpoints $\phi_{k-\frac{1}{2}}$, $k = 1, \ldots, N$, and the integrals are approximated using Simpson's rule. After interpolation and the inversion of a matrix, a linear system of the form

$$\xi_i' = \tfrac{1}{2} + \sum_{j=1}^{N} H_{ij}\,\eta_j' + H_{i,\,N+1}(\xi_0' - \tfrac{1}{2}) + H_{i,\,N+2}\,\eta_0' \quad (i = 1, \ldots, N) \tag{4.1}$$

is obtained, where the constants H_{ij}, $i = 1, \ldots, N$, $j = 1, \ldots, N+2$ are all known.

Since all the flow quantities at the first point ϕ_0 are assumed known, Gregory's Rule integration is used to obtain the values of ξ and η at the free-surface points. For example

$$\xi_i = \xi_0 + \sum_{j=0}^{N} a_{ij}\,\xi_j' \quad (i = 1, \ldots, N). \tag{4.2}$$

Lagrangian five-point differentiation formulae are used to obtain the second derivatives ξ'' and η''. Thus

$$\xi_i'' = \sum_{j=0}^{N} b_{ij}\,\xi_j' \quad (i = 1, \ldots, N), \tag{4.3}$$

for suitable weights a_{ij}, b_{ij}. Similar formulae hold for the computation of η and η'' at the free-surface points.

The Bernoulli equation (2.7), evaluated at the points $\phi_1, \ldots, \phi_N$, yields a system of N nonlinear algebraic equations of the form

$$P_i(\eta_1', \ldots, \eta_N') = 0 \quad (i = 1, \ldots, N), \tag{4.4}$$

where the functions ξ, η, ξ', ξ'', η'' have been eliminated in favour of values of η' at the indicated free-surface points by means of (4.1)–(4.3). The functions P_i are the residual surface pressures at the points ϕ_i, $i = 1, \ldots, N$. Equations (4.4) are solved by a Newton–Raphson process, using forward differences to approximate the derivatives in the Jacobian matrix. With $N = 130$ a converged nonlinear solution is usually obtained from the linearized result in about five iterations. Occasionally, however, it is necessary to use a previously computed nonlinear solution as the starting guess in the Newton scheme, in order to obtain convergence.

Once the solution is known at the free surface $\psi = 1$, the drag D may be computed using Cauchy's Integral Theorem to generate values of ξ' at the bottom $\psi = 0$. These values are integrated to obtain ξ, and (2.12) are solved using cubic spline interpolation and Newton's method. The drag D is then found from (2.11) by Simpson's Rule integration.

5. Presentation of results

5.1. *Solutions of type* 1

Three nonlinear solutions of type 1 have been computed for $F = 0{\cdot}8$, $\alpha = 0{\cdot}05$ and are shown in figure 3. As the surface-tension parameter T is increased, the wavelength of the downstream waves decreases significantly. This result is also predicted by the linearized solution, since κ_0 increases with increasing T. The amplitude of the upstream and downstream waves increases with increasing T, as is the case for the linearized solution; however, unlike the linearized solution, the mean free-surface level for the nonlinear downstream wavetrains shown in figure 3 evidently lowers as T is made larger.

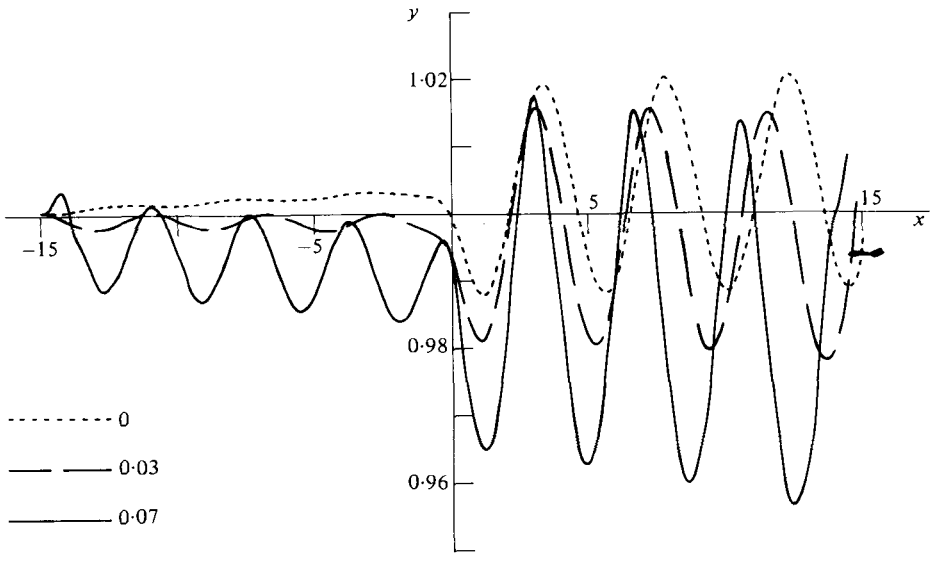

FIGURE 3. Three nonlinear solutions of type 1, for $F = 0{\cdot}8$ and $\alpha = 0{\cdot}05$. Results are shown for the three values of the surface-tension parameter $T = 0$, 0·03 and 0·07.

The problems associated with the computation of nonlinear free-surface profiles by the present method in the absence of surface tension ($T = 0$) have been described previously by Forbes & Schwartz (1982). In general it is found that the truncation of the integrodifferential equation downstream at the last point ϕ_N results in an unimportant error which affects only the last quarter wavelength or so downstream. The upstream truncation at $\phi = \phi_0$ and the subsequent imposition of the radiation condition (2.9) there gives rise to a spurious upstream wavetrain of small amplitude. By specifying the 'correct' values of η_0, ξ_0, etc. to be imposed there, this spurious wavetrain may be eliminated; in particular, nonlinear effects evidently result in a local rise in the free-surface level ahead of the obstacle, so that, by increasing the value of η_0 slightly above the value suggested by (2.9), the amplitude of the spurious upstream waves may be made very small indeed. This procedure was adopted to eliminate almost completely the spurious upstream waves for the $T = 0$ case shown in figure 3.

Although the numerical problems associated with the upstream and downstream truncation of the integrodifferential equation (2.8) have been successfully overcome for the special case $T = 0$ as described above, this truncation becomes an important concern in the computation of the general solution of type 1 in which surface tension is present. As T is increased, the portion of the downstream wavetrain affected by the downstream truncation becomes greater. Thus for the solution with $T = 0{\cdot}03$ shown in figure 3, the last wavelength downstream is in error. For $T = 0{\cdot}07$, which is the largest value of T for which Newton's method converged, the error extends over the last two wavelengths downstream. The upstream truncation is also of concern, since the behaviour of $\zeta(f)$ as $\phi \to -\infty$ is not known, so that the values of the flow variables to be imposed at $\phi = \phi_0$ are unclear. Of course, this information could be obtained by continuing the series expansion (3.1) out to higher orders in α^2; however, this would appear to be a prohibitively complicated process, and no attempt has been made to pursue this further. For the solutions shown in figure 3, the value of η_0 imposed at the first point ϕ_0 was chosen to be that value which

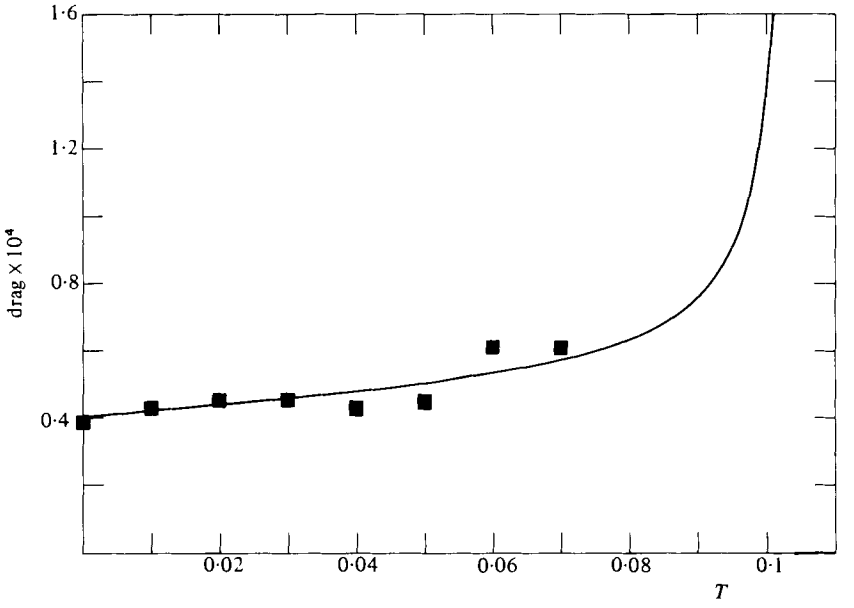

FIGURE 4. Drag as a function of surface-tension parameter, for $F = 0{\cdot}8$, $\alpha = 0{\cdot}05$. The curve is the result of linearized theory, and the points denote nonlinear results.

eliminated the spurious upstream waves for the $T = 0$ case. The values of the quantities ξ_0, η_0', ξ_0'' and η_0'' were taken from the linearized solution, and ξ_0' was then found from the Bernoulli equation. Despite the obvious shortcomings of this approximation, free-surface profiles are nevertheless obtained which are reasonably insensitive to the positions of the truncation boundaries and to further reductions in the spacing between free-surface points.

The drag on the semicircle as a function of the surface-tension parameter T is shown in figure 4, for the same values of Froude number and semicircle radius as in figure 3. The linearized result, calculated from (3.6), is shown as a solid curve, and the points are the values of the drag determined from converged nonlinear free-surface profiles by the method described at the end of §4. The linearized and nonlinear results agree closely over the entire range of values of T for which Newton's method converged. The slight scatter in the nonlinear values about the linearized result at the larger values of T is undoubtedly a consequence of numerical errors of the type described above, which become more severe as T is increased.

Figure 5 shows the values of α and T for which linearized solutions of types 1 and 2 exist, and nonlinear solutions of both types may be found by the present method, when $F = 0{\cdot}5$. In the linearized theory, solutions of type 1 are predicted in the region to the left of the dashed line at $T = 0{\cdot}0156$, and solutions of type 2 are predicted for $T > 0{\cdot}0156$. When $T = 0{\cdot}0156$, there is no solution. This linearized theory is only strictly valid as $\alpha \to 0$, so that the vertical axis in figure 5 indicates the effects of nonlinearity directly.

The values of α and T for which nonlinear solutions may be obtained appear to be restricted to values lying roughly within the regions bounded by the solid lines sketched in figure 5. Nonlinear solutions of type 1 are thus confined to the approximately triangular-shaped region in the bottom left-hand corner of figure 5. The six points within this region represent the largest values of T for which Newton's method converged to a nonlinear solution of type 1, for six different values of α.

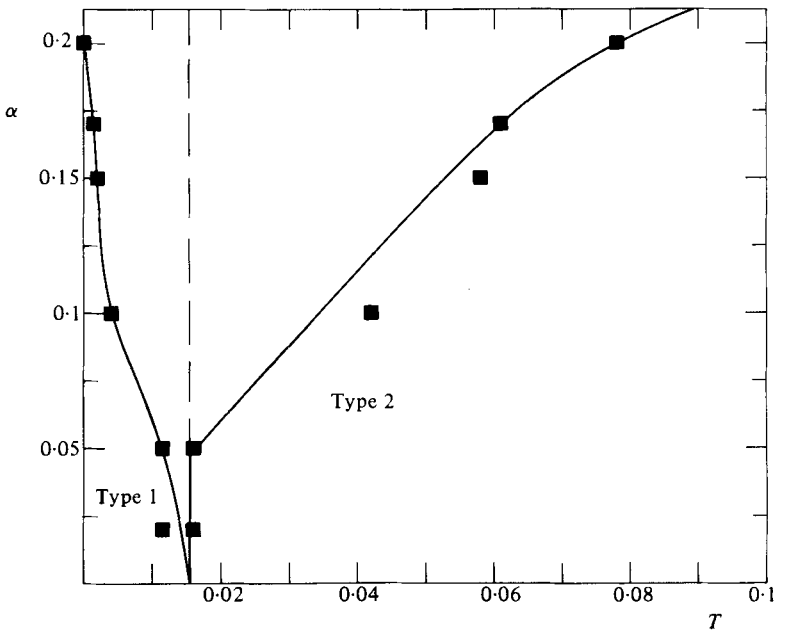

FIGURE 5. The regions in the (α, T) parameter space in which solutions of types 1 and 2 may be found, when $F = 0{\cdot}5$. The dashed line separates linearized solutions of types 1 and 2. The points represent extreme values of T for which Newton's method converged in the nonlinear case, for solutions of both types.

Nonlinear type 2 solutions, to be discussed later, appear to exist only in the region to the right of the second solid line in figure 5; the six points within this region indicate the smallest values of T for which Newton's method converged. In view of the relatively small number of free-surface points (about 20 points per wave cycle) to which we are restricted by the storage limits of the computer, it has not been possible to determine the nature of the physical processes responsible for limiting the size of the region in figure 5 within which solutions of type 1 exist, since Newton's method fails to converge when the curvature of the free surface becomes too great.

In figure 6 the dependence of the drag upon the surface-tension parameter T is shown for a semicircle of radius $\alpha = 0{\cdot}05$ in a flow with $F = 0{\cdot}5$. The linearized result, shown as a solid curve, indicates a monotonic decrease in the drag as T is increased, followed by an abrupt rise near the critical value $T = 0{\cdot}0156$. The nonlinear results suggest a slight increase in drag with increasing T, followed by a region in which the drag decreases. Newton's method fails to converge at a value of T considerably smaller than the critical value $T = 0{\cdot}0156$ for the linearized solution, and the nonlinear results also indicate an abrupt rise in the drag at this value of T.

5.2. *Solutions of type* 2

According to the linearized theory, solutions of type 2 are predicted to occur in subcritical flow ($F < 1$) when the surface-tension parameter T exceeds a certain critical value (see figure 2). The free surface is symmetric about $x = 0$, and consists of a single depression above the semicircle.

The values of T for which nonlinear solutions of type 2 may be found have been presented in figure 5, for $F = 0{\cdot}5$. For $\alpha \gtrsim 0{\cdot}05$, nonlinear solutions appear to exist only in the region to the right of the line sketched on the figure. When $0 < \alpha < 0{\cdot}05$,

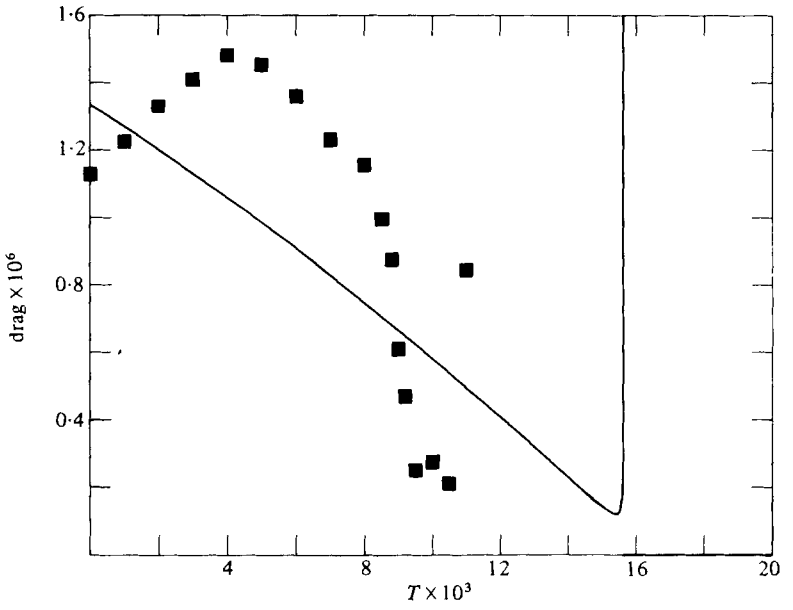

FIGURE 6. Drag as a function of surface-tension parameter T, when $F = 0{\cdot}5$ and $\alpha = 0{\cdot}05$. The smooth curve is the linearized result, and the points denote nonlinear values.

however, the situation is possibly of greater interest. Here, our numerical method failed to converge to a nonlinear solution of type 2 for $T < 0{\cdot}0156$, which is the critical value for the linearized solution. However, numerical errors due to the truncation of the integrodifferential equation (2.8) downstream at the point ϕ_N become very large for type 2 solutions as $T \to 0{\cdot}0156$, and may perhaps prevent the convergence of Newton's method for $T < 0{\cdot}0156$. The possibility that nonlinear solutions of type 2 might exist for $T < 0{\cdot}0156$ certainly cannot be dismissed, so that, in a portion of the parameter space shown in figure 5, nonlinear solutions of types 1 and 2 might perhaps exist simultaneously. Such a lack of uniqueness in the solutions to this problem would be similar to the situation described by Forbes & Schwartz (1982).

The shape of the free surface for two nonlinear solutions of type 2, obtained with $F = 0{\cdot}5$ and $\alpha = 0{\cdot}17$, is shown in figure 7. The upward inflexion in the free-surface profile at $x \approx 6$ for the $T = 0{\cdot}2$ case is a numerical error caused by the downstream truncation of the integrodifferential equation at $\phi = \phi_N$. The solution for $T = 0{\cdot}061$ exhibits a much sharper trough at $x = 0$ than occurs at $T = 0{\cdot}2$, and represents the smallest value of T for which Newton's method converged to a nonlinear type 2 solution. Again, the physical process responsible for the failure of Newton's method for type 2 solutions with $T < 0{\cdot}061$ is not clear from our results, but is presumably related to the large curvature at the trough. It is possible that the free surface might enclose a bubble at the trough for $T \approx 0{\cdot}06$.

5.3. *Solutions of type* 3

Nonlinear solutions of type 3 in the absence of surface tension have been discussed in detail by Forbes & Schwartz (1982). They occur in a portion of the supercritical flow regime $F > 1$, the extent of which depends upon the circle radius α, and the free-surface profile consists of a single elevation above the semicircle. There appears to be a maximum value of the circle radius α at which solutions may be found, for a given value of F; at this value of α, the free surface presumably forms a sharp crest above the semicircle, with sides that enclose an angle of 120°.

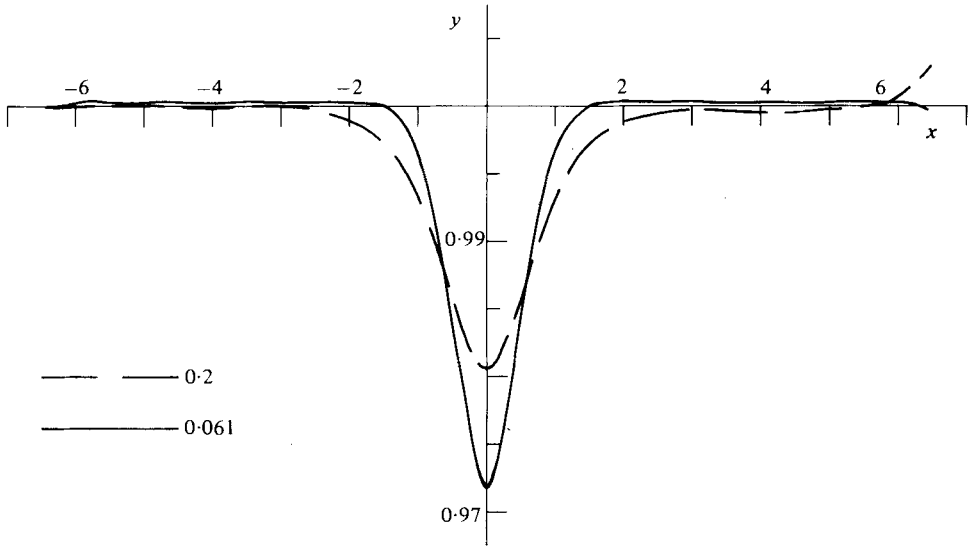

FIGURE 7. Two nonlinear solutions of type 2, for $F = 0{\cdot}5$ and $\alpha = 0{\cdot}17$, at the two different values of the surface-tension parameter $T = 0{\cdot}061$ and $0{\cdot}2$.

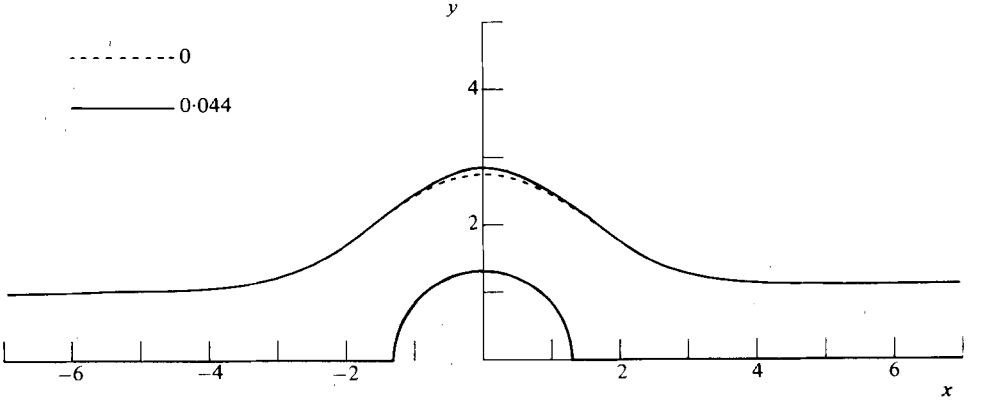

FIGURE 8. Two nonlinear solutions of type 3, for $F = 2{\cdot}1$ and $\alpha = 1{\cdot}32$. The free surface is shown in the absence of surface tension, and for $T = 0{\cdot}044$.

Two nonlinear type 3 solutions are shown in figure 8, for the case $F = 2{\cdot}1$, $\alpha = 1{\cdot}32$. This is the largest value of α at which Newton's method converged, for the solution with $T = 0$. The introduction of surface tension appears to have only slight effects on the free-surface profile. The linearized theory predicts upstream capillary waves of very small amplitude for $T \neq 0$, although no evidence of these exists in the nonlinear results. The maximum free-surface elevation for the $T = 0{\cdot}044$ case is slightly greater than that obtained in the absence of surface tension. Newton's method fails to converge for $T > 0{\cdot}044$, so that our results are unable to indicate the nature of the influence of surface tension upon the formation of a crest at the free surface.

6. Summary and discussion

Two-dimensional flow of an ideal fluid over a submerged semicircular cylinder has been discussed. The fluid is subject to the combined effects of gravity and surface tension.

The linearized theory, derived under the assumption that the semicircular cylinder is of small radius, predicts the existence of three different types of solution, which have been referred to here as being of types 1 to 3. Solutions of type 1 possess an upstream capillary wavetrain, followed by a train of gravity waves downstream of the semicircle, and the free surface for type 2 solutions consists of a single depression above the obstacle. Type 3 solutions possess an upstream capillary wavetrain and an elevation of the free surface in the vicinity of the semicircular obstruction.

The solution of the fully nonlinear problem confirms the existence of the above three classes of solution. For each class the ability of the present numerical scheme to compute solutions is ultimately limited by the formation of regions of very high curvature at the free surface. In the case of type 1 solutions these regions are presumably associated either with wave breaking at the crests, when the semicircle radius is large, or with the formation of bubbles enclosed by the troughs, for large surface tension. Nonlinear solutions of type 2 are most likely limited by the trapping of a bubble at the free surface in the region above the semicircle, for a suitably small value of the surface tension, and the failure of type 3 solutions is apparently associated with the formation of a crest at the surface, immediately above the semicircular obstruction.

In the linearized theory the values of the flow parameters F, α and T uniquely specify which of the three branches of solution will result. However, this apparently ceases to be true of the nonlinear solution. The possibility of overlap between solutions of types 1 and 3 has already been discussed by Forbes & Schwartz (1982), and the results presented in this paper suggest a possible overlap between solutions of types 1 and 2.

In addition to non-uniqueness of solutions due to overlap of the various different branches, there are presumably also *infinitely many* different kinds of solution of type 1. This is a consequence of the existence of 'Wilton's ripples' in the nonlinear solution, as described in §1. A countably infinite spectrum of solutions of type 1 is therefore to be expected, such that the waves downstream of the obstacle may generally possess a characteristic number of 'dimples' per wavelength. Such solutions have not yet been observed with the present numerical scheme; however, this is not at all surprising, in view of the small number of free-surface points per wavelength to which we are presently restricted.

To conclude, some remarks on the physical plausibility of the solutions obtained in this paper are appropriate. Forbes & Schwartz (1982) suggest that the existence of type 3 solutions is doubtful; presumably such supercritical solutions are unstable, and degenerate into configurations involving an hydraulic jump. Type 2 solutions would not normally be seen in water, although they could occur in fluids with enhanced surface tension, such as an oil slick close to the shore. The existence of type 1 solutions is not in doubt, although the capillary waves do not propagate *infinitely far* upstream of the semicircle. In fact, for water, the effects of surface tension on the upstream portion of the flow are of the same order of magnitude as the effects of fluid viscosity, so that substantial damping of the upstream wavetrain may be expected.

This work was commenced whilst the author was in receipt of an Australian Postgraduate Research Award, and was completed under Australian Research Grants Committee grant number F76/15343R, at the University of Adelaide.

REFERENCES

AITCHISON, J. M. 1979 A variable finite element method for the calculation of flow over a weir. *Rutherford Lab. Rep.* RL-79-069.

CHEN, B. & SAFFMAN, P. G. 1979 Steady gravity–capillary waves on deep water – I. Weakly nonlinear waves. *Stud. Appl. Math.* **60**, 183–210.

CHEN, B. & SAFFMAN, P. G. 1980 Steady gravity–capillary waves on deep water – II. Numerical results for finite amplitude. *Stud. Appl. Math.* **62**, 95–111.

COKELET, E. D. 1977 Steep gravity waves in water of arbitrary uniform depth. *Phil. Trans. R. Soc. Lond.* A **286**, 183–230.

FORBES, L. K. 1981*a* On the wave resistance of a submerged semi-elliptical body. *J. Engng Maths* **15**, 287–298.

FORBES, L. K. 1981*b* Non-linear, drag-free flow over a submerged semi-elliptical body. *J. Engng Maths* (to appear).

FORBES, L. K. & SCHWARTZ, L. W. 1982 Free-surface flow over a semicircular obstruction. *J. Fluid Mech.* **114**, 299–314.

GAZDAR, A. S. 1973 Generation of waves of small amplitude by an obstacle placed on the bottom of a running stream. *J. Phys. Soc. Japan* **34**, 530–538.

HAUSSLING, H. J. & COLEMAN, R. M. 1977 Finite-difference computations using boundary-fitted coordinates for free-surface potential flows generated by submerged bodies. In *Proc. 2nd. Int. Conf. on Numerical Ship Hydrodynamics, Berkeley*, pp. 221–233.

HOGAN, S. J. 1979 Some effects of surface tension on steep water waves. *J. Fluid Mech.* **91**, 167–180.

HOGAN, S. J. 1980 Some effects of surface tension on steep water waves. Part 2. *J. Fluid Mech.* **96**, 417–445.

KERCZEK, C. VON & SALVESEN, N. 1977 Non-linear free-surface effects – the dependence on Froude number. In *Proc. 2nd Int. Conf. on Numerical Ship Hydrodynamics, Berkeley*, pp. 292–300.

LAMB, H. 1932 *Hydrodynamics*, 6th edn. Cambridge University Press.

SCHWARTZ, L. W. 1974 Computer extension and analytic continuation of Stokes' expansion for gravity waves. *J. Fluid Mech.* **62**, 553–578.

SCHWARTZ, L. W. & VANDEN BROECK, J.-M. 1979 Numerical solution of the exact equations for capillary–gravity waves. *J. Fluid Mech.* **95**, 119–139.

SHANKS, S. P. & THOMPSON, J. F. 1977 Numerical solution of the Navier–Stokes equations for 2D hydrofoils in or below a free surface. In *Proc. 2nd Int. Conf. on Numerical Ship Hydrodynamics, Berkeley*, pp. 202–220.

STOKES, G. G. 1880 *Mathematical and Physical Papers*, vol. 1. Cambridge University Press.

WEHAUSEN, J. V. & LAITONE, E. V. 1960 Surface waves. In *Handbuch der Physik*, vol. 9. Springer.